The Visual Computer (2019) 35:949–959
https://doi.org/10.1007/s00371-019-01672-z

ORIGINAL ARTICLE

A lightweight methodology of 3D printed objects utilizing multi-scale porous structures

Jiangbei Hu[1] · Shengfa Wang[1] · Yi Wang[1] · Fengqi Li[1] · Zhongxuan Luo[1,2]

Published online: 6 May 2019

Abstract
Lightweight modeling is one of the most important research subjects in modern fabrication manufacturing, and it provides not only a low-cost solution but also functional applications, especially for the fabrication using 3D printing. This approach presents a multi-scale porous structure-based lightweight framework to reduce the weight of 3D printed objects while meeting the specified requirements. Specifically, the triply periodic minimal surface (TPMS) is exploited to design a multi-scale porous structure, which can achieve high mechanical behaviors with lightweight. The multi-scale porous structure is constructed using compactly supported radial basis functions, and it inherits the good properties of TPMS, such as smoothness, full connectivity (no closed hollows) and quasi-self-supporting (free of extra supports in most cases). Then, the lightweight problem utilizing the porous structures is formulated into a constrained optimization. Finally, a strength-to-weight optimization method is proposed to obtain the lightweight models. It is also worth noting that the proposed porous structures can be perfectly fabricated by common 3D printing technologies on account of the leftover material, such as the liquid in SLA, which can be removed through the fully connected void channel.

Keywords Lightweight · Porous structures · 3D Printing

1 Introduction

3D printing technologies bring vitality to modern manufacturing and receive considerable attention in engineering and academic fields. Lightweight modeling is one of the most important and challenging topics in energy conservation and environmental protection and is widely used in automobile, aviation, medicine and many other fields. However, it is still a task of great challenge to design strong and lightweight structures under the given conditions. This impels us to design lightweight porous structures for 3D printed objects.

Various interior structures or supports have been proposed to gain the lightweight objects. Hollowing the 3D objects is a straightforward method that could make the models lighter while sustaining the external loads [1]. As reported, using honeycomb-like structures is also effective way to achieve the lightweight purpose [2]. The skin-frame structures are widely used in architecture, and they are also a positive option as internal supports for cost-effective models [3]. Similar to the frame structures, medial axis tree can also be used to reduce the weight [4]. This work has made great contributions to the optimization of lightweight objects. Different from the previous work, we exploit TPMS to construct multi-scale porous structures, which are used as the lightweight interior supports of the 3D models. The multi-scale porous structures inherit the good properties of TPMS, including smoothness, controllability, full connectivity and quasi-self-supporting. The TPMS-based porous structures have been reported that they have very good performances on scaffold architectures in many fields [5–7]. Drawing inspiration from this, we construct a multi-scale porous structure utilizing the compactly supported radial basis functions and apply it to the lightweight modeling of 3D printed objects.

We propose a multi-scale porous structure-based lightweight framework to obtain strong and lightweight 3D printed models, and the main procedure is shown in Fig. 1. Specifically, given a 3D model and the specified physical conditions (such as external loads, gravity and material), we first calculate an initial stress field, and then a volume partition can

✉ Shengfa Wang
sfwang@dlut.edu.cn

Zhongxuan Luo
zxluo@dlut.edu.cn

[1] Dalian University of Technology, Dalian, China

[2] Guilin University of Electronic Technology, Guilin, China

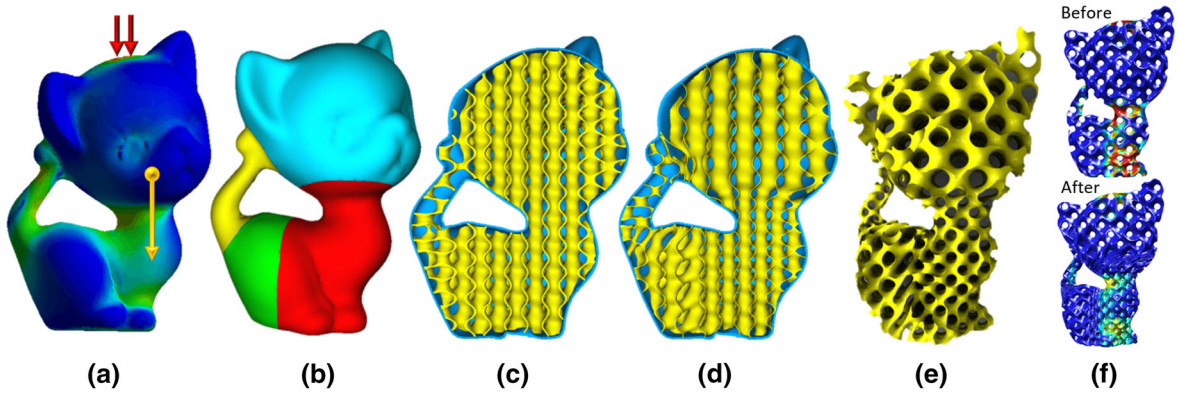

Fig. 1 Illustration of the proposed lightweight framework. **a** Kitty model with initial stress field. **b** Stress-field-guided volume partition. **c**, **d** Optimum iterative procedure. **e** Optimized interior porous structures. **f** Stress analysis before and after optimization, respectively

be obtained according to the stress field. After that, we formulate our lightweight framework into a constraint optimization with two parameters and solve the optimization problem by a stress-to-weight algorithm. In addition, the lightweight objects we constructed have types of advantages, including the smoothness, the controllability, the full connectivity and the quasi-self-supporting. The quasi-self-supporting means that the internal structures of the lightweight models are almost free of extra supports for the common 3D printing technologies (details will be discussed in Sect. 3.2), and the full connectivity guarantees that the leftover of the material (such as liquid in DLP and SLA, particles in SLS) can be removed. Therefore, the porous structure is suitable for most of the common 3D printing technologies (such as FDM, DLP, SLA, SLS and so on). The porous structures can be manufactured using FDM technology without extra supports in all our experiments. The primary contributions can be summarized as follows:

- We devise a novel TPMS-based multi-scale porous structure, which can be easy to operate for both topological (porous period) and geometric (wall thickness) changes. Moreover, the proposed porous structures are smooth, fully connected and quasi-self-supported and can be manufactured using common 3D printing technologies.
- We adapt the proposed porous structure to lightweight framework with only two parameters and provide a credible strength-to-weight optimization to solve the lightweight problem. The optimized results have smooth and natural transition of changes and maintain good properties of the porous structures.

2 Related work

With the rapid development of 3D printing technologies, lightweight modeling and optimization have received considerable attention. We list the related methods from three aspects, including lightweight modeling, porous structures and structure optimization.

Lightweight modeling Lightweight modeling has been extensively explored in computer-aided design and tissue engineering. The most direct idea is hollowing, which is widely used in many fields, especially for 3D printing [8]. Stava et al. [1] presented a method of enhancing the strength of printed models by hollowing, thickening and adding extra trusses. Similarly, Lu et al. [2] introduced a hollowing optimization algorithm based on honeycomb-like structures, which were computed based on the stress distribution. However, the hollowed cells in their method are closed, and they are not suitable for some common 3D printing technologies (such as SLS and DLP). There were also some similar ways that used lightweight structures to improve the strength of models in earlier years [9,10]. Wang et al. [3] proposed a frame structure to reduce the material in 3D printing by formulating the problem as a multi-objective optimization. Later, several similar structures, such as stiffness structure and medial axis tree, were exploited to address this issue [4,11].

Infilling structure design Thanks to the development of 3D printing manufacturing technologies [12], complex infilling structures can be designed to meet various needs in engineering fields. Several types of porous scaffolds were designed to meet the practical requirements, such as foams-like structures [13], lattice structures [3,4], honeycomb-cell structures [2] and so on [14–17]. More interesting structures can be found in the review [18]. Among these various infilling structures, TPMS-based porous structures have got more and more attention because of its excellent inherent properties [19–22]. Triply periodic minimal surface (TPMS) is a kind of minimal surfaces that can extend periodically and indefinitely in the space [23]. Compared to other porous structures, the TPMS-based structures have several advantages, including easy controllability, high smoothness, full continuity, quasi-

self-supporting and universal adaptability of the common 3D printing technologies. Rajagopalan et al. [6] presented the first practical application of TPMS to construct the scaffolds. Many studies have shown that TPMS has a good performance in mechanical properties [24]. Yoo et al. [7,25] proposed a modeling algorithm that combines Volume Distance Field and Boolean operation, which made it easy to build the internal structure for arbitrary shape of objects. They exploited the radial basis functions [26] to control the internal scaffold architecture. However, the previously proposed TPMS-based porous structures were almost heuristic and straightforward applications without optimization, and there were more or less problems of smoothness, connectivity or controllability. Later, Li et al. [27,28] designed TPMS-based functionally graded cellular structures with thickness changes for additive manufacturing. However, only geometric (thickness) changes are considered, but the topological optimization is not applied. Drawing inspiration from this work, we creatively use the radial basis function with compact support set [29] to construct the multi-scale porous structure with smooth topological and geometric changes.

Structure optimization Structure optimization is also a related research subject. Many algorithms were proposed to improve the structure attributes of 3D models [30], such as structure strength [1,31,32] and balance [33] and support-free design [34,35]. The static or dynamic behaviors could be adjusted through the structural optimization [36–39]. The topology optimization could also be used to construct lightweight and high-resistance structures [40]. There are several well-known approaches for topology optimization, such as Solid Isotropic Material with Penalization (SIMP) [41], the level set method [42] and the evolutionary method [43]. However, there are common problems with these methods: For example, finding a precise solution costs a lot and the number of variables is relatively large. As a result, they execute topology optimization in an implicit way. To solve this, an explicit method called the Moving Morphable Components (MMCs) was proposed [44]. There are still a lot of other works on structural and topology optimization of 3D objects [45,46]. Note that lightweight work [2–4] including our method belongs to the structure optimization, but we focus more on the strength-to-mass optimization.

3 TPMS-based porous structure

Triply periodic minimal surfaces (TPMS) could be used to construct a 'like-natural' porous structure. As one kind of minimal surfaces, the mean curvature of TPMS vanishes at every point. Moreover, TPMS can extend periodically and indefinitely in three independent directions to construct a controllable porous structure.

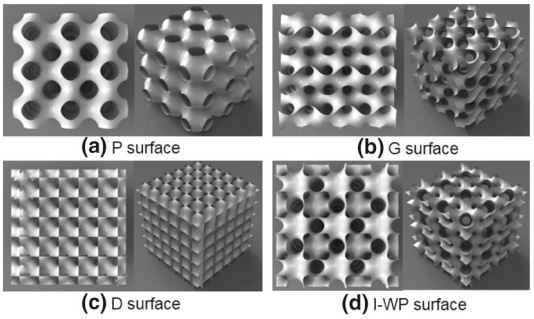

Fig. 2 Four kinds of common TPMS surfaces

3.1 The description of TPMS

The TPMS can be expressed as

$$\phi(\mathbf{r}) = \sum_{k=1}^{K} A_k \cos[2\pi(\mathbf{h}_k \cdot \mathbf{r})/\lambda_k + P_k] = C, \tag{1}$$

where $\mathbf{r}$ is a location vector, A_k is a magnitude factor, $\mathbf{h}_k$ is the k-th lattice vector, λ_k is the wavelength of periods, P_k is the phase shift and C is a constant value (it is a minimal surface when $C = 0$), as defined in [23].

The TPMS can also be approximated by periodic surfaces. There are some kinds of TPMS that are frequently used in chemistry and materialogy, such as P surface, G surface, D surface and I-WP surface as shown in Fig. 2. These four kinds of surfaces can be re-expressed as follows:

$$\begin{aligned}
\phi_P(\mathbf{r}) &= \cos(2\pi x) + \cos(2\pi y) + \cos(2\pi z) = C,\\
\phi_G(\mathbf{r}) &= \sin(2\pi x)\cos(2\pi y) + \sin(2\pi z)\cos(2\pi x)\\
&\quad + \sin(2\pi y)\cos(2\pi z) = C,\\
\phi_D(\mathbf{r}) &= \cos(2\pi x)\cos(2\pi y)\cos(2\pi z)\\
&\quad - \sin(2\pi x)\sin(2\pi y)\sin(2\pi z) = C,\\
\phi_{I-WP}(\mathbf{r}) &= 2[\cos(2\pi x)\cos(2\pi y) + \cos(2\pi y)\cos(2\pi z)\\
&\quad + \cos(2\pi z)\cos(2\pi x)] - [\cos(2\cdot 2\pi x)\\
&\quad + \cos(2\cdot 2\pi y) + \cos(2\cdot 2\pi z)] = C.
\end{aligned} \tag{2}$$

3.2 The construction of multi-scale porous structures

We utilize the TPMS to construct a multi-scale porous structure that will be further applied to our lightweight framework. As shown in Fig 3a, we verified that the parameter C has small impact on strength-to-volume ratio. Moreover, when $C = 0$, the corresponding porous surface has better smoothness and uniformity. Therefore, the parameter C is fixed to zero in the approach.

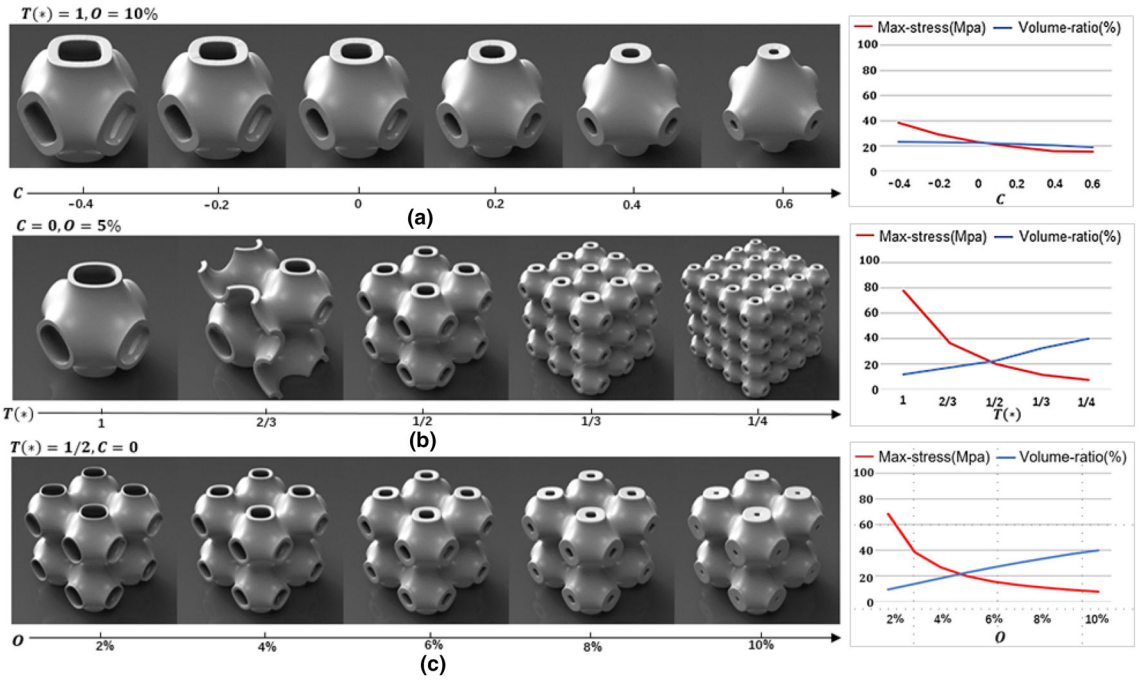

Fig. 3 Effect of different parameters (**a** shape parameter C, **b** period parameter $T(*)$, and **c** offset parameter O) on the porous structures (P surface), and the corresponding parameter curves (under the same external force conditions, max stress means the max stress of the structures, and volume ratio is the volume ratio of the structures to the bounding box). The period parameter $T(*)$, and the offset parameter O have similar monotonic effects on the max stress and volume ratio

For convenience, P surface will be taken as an example to illustrate the proposed method, and other kinds of TPMS can be processed in the same way. In order to construct a multi-scale P surface, a control function of porous period should be introduced

$$\widetilde{\phi}_P(\mathbf{r}) = \cos\left(\frac{2\pi x}{T(\mathbf{r})}\right) + \cos\left(\frac{2\pi y}{T(\mathbf{r})}\right) + \cos\left(\frac{2\pi z}{T(\mathbf{r})}\right) = 0, \tag{3}$$

where $\mathbf{r} \in R^3$ is location vector with Cartesian coordinates (x, y, z), and $T(\mathbf{r}) > 0$ is a control function of porous period (density distribution) that should be a continuous distribution of the period values in space (as shown in Fig. 3b). The period control function $T(\mathbf{r})$ can be approximated using compactly supported radial basis function (CSRBF) as

$$T(\mathbf{r}) = \sum_{i=1}^{m} \omega_i \varphi(||\mathbf{r} - \mathbf{c}_i||) + Q(\mathbf{r}), \tag{4}$$

where $\{\mathbf{c}_i\}$ are control points with specified $T(\mathbf{c}_i) = T_i$, m is the number of control points ($m = 300$ by default), $\varphi(*)$ is a CSRBF, $\{\omega_i\}$ are the corresponding weights and $Q(\mathbf{r}) = q_0 + q_1 x + q_2 y + q_3 z$.

The weights $\{\omega_i\}$ and $Q(\mathbf{r})$ can be solved by a linear system

$$\begin{bmatrix} \varphi_{11} & \varphi_{12} & \cdots & \varphi_{1m} & 1 & c_1^x & c_1^y & c_1^z \\ \varphi_{21} & \varphi_{22} & \cdots & \varphi_{2m} & 1 & c_2^x & c_2^y & c_2^z \\ \vdots & \vdots & \ldots & \vdots & \vdots & \vdots & \vdots & \vdots \\ \varphi_{m1} & \varphi_{m2} & \cdots & \varphi_{mm} & 1 & c_m^x & c_m^y & c_m^z \\ 1 & 1 & \cdots & 1 & 0 & 0 & 0 & 0 \\ c_1^x & c_2^x & \cdots & c_m^x & 0 & 0 & 0 & 0 \\ c_1^y & c_2^y & \cdots & c_m^y & 0 & 0 & 0 & 0 \\ c_1^z & c_2^z & \cdots & c_m^z & 0 & 0 & 0 & 0 \end{bmatrix} \begin{bmatrix} \omega_1 \\ \omega_2 \\ \vdots \\ \omega_m \\ q_0 \\ q_1 \\ q_2 \\ q_3 \end{bmatrix} = \begin{bmatrix} T_1 \\ T_2 \\ \vdots \\ T_m \\ 0 \\ 0 \\ 0 \\ 0 \end{bmatrix}, \tag{5}$$

where (c_i^x, c_i^y, c_i^z) is the Cartesian coordinates of control point $\mathbf{c}_i$, $\varphi_{ij} = \varphi(\| \mathbf{c}_i - \mathbf{c}_j \|)$ is the radial basis function between $\mathbf{c}_i$ and $\mathbf{c}_j$.

In the approach, we chose the radial basis function with compact support set as

$$\varphi(t) = \begin{cases} (\frac{\alpha - t}{\alpha})^6 [32(\frac{t}{\alpha})^3 + 25(\frac{t}{\alpha})^2 + 8\frac{t}{\alpha} + 1] & \text{if } t < \alpha, \\ 0 & \text{otherwise.} \end{cases} \tag{6}$$

where α is the radius of the support set (1/5 the length of the bounding box by default). Compared to other radial basis functions, such as thin-plate function, Gaussian function and so on, there are two advantages of the CSRBF: the control-

lable affected regions of control points and the sparsity of the CSRBF. The former can reduce the erroneous interpolation caused by some uncorrelated control points, and the latter could make the matrix in Eq. (5) sparse, which lowers the computational complexity.

The multi-scale porous structure filling arbitrary shape of 3D model M can be designed using the Volumetric Distance Field (VDF) and Boolean operations [25]

$$\phi_M = \widetilde{\phi}_{\text{TPMS}} \cap \phi_{\mathcal{S}} = \min(\widetilde{\phi}_{\text{TPMS}}, \phi_{\mathcal{S}}), \tag{7}$$

where $\widetilde{\phi}_{\text{TPMS}}$ is the multi-scale TPMS surface, and $\phi_{\mathcal{S}}$ is the VDF representing the shape of M. Therefore, the porous surface ϕ_M constitutes the interior structure of M by specifying a proper offset O (wall thickness, the percentage of the longest edge of the bounding box, as shown in Fig. 3c). The porous period parameter $T(*)$ and the offset O will be optimized in our lightweight framework.

The proposed porous structures inherit various good properties of the TPMS, such as the smooth surface of structures, high controllability, fully connected hollows (no closed hollows) and quasi-self-supporting. Particularly, the properties of fully connected hollows and quasi-self-supporting ensure the porous structures are printable. As shown in Fig. 4, two regions with control points are specified in a cube, and a corresponding multi-scale P surface is obtained with smooth and natural transition regions. Figure 5 shows the examples of supporting angles on P surface and G surface, and we can see that the angles of the most regions are less than 45°, which are free of supports. Moreover, due to the smoothness and the saddle surface of the structures, they actually do not need extra supports. In our experiments, the porous structures are printed using FDM-based 3D printer without extra supports.

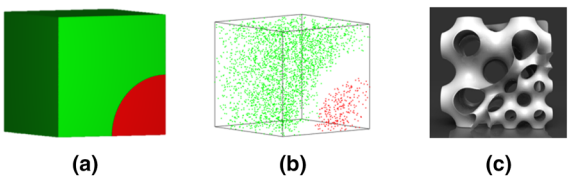

Fig. 4 Multi-scale porous structures in a cube. **a** Cube model with a partition. **b** Two types of control points with different T_i are randomly selected in the two regions, respectively. **c** The multi-scale porous structures

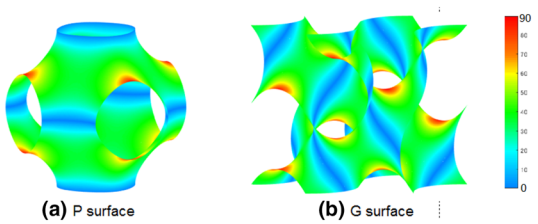

Fig. 5 Angles between faces and the printing direction. **a**, **b** P surface and G surface with 19.1% and 23.1% of the angles are larger than 45°, and only 5.2% and 8.4% of the angles are larger than 60°, respectively

4 The lightweight framework based on porous structures

Given a 3D model $\mathcal{M}$ and the external forces conditions, our goal is to yield a supportive interior porous structure with proper period parameter $T(*)$ and offset parameter O, which has minimal weight of material while can resist the external forces and imposed interior load.

4.1 Problems and strategies

Parameters The period parameter $T(*)$ controls the period distribution of the porous structures, and the offset parameter O controls the wall thickness of the porous structures. Essentially, both parameters cooperatively govern the mass distribution of interior structures and the strength. We can also see in Fig. 3, both parameters have the similar influence on the strength-to-weight ratio (the relative slope of max stress and volume rate), i.e., as the offset/period parameter increases/decreases, the porous structures become heavier and stronger. Besides, $\{T(*)\}$ has a larger available range of changes and is more flexible than O (non-self-intersection, porous connectivity). Therefore, we treat the offset parameter O as a constant value optimization and release the period parameter $T(*)$ to obtain an optimized strength-to-weight ratio. It could reduce the complexity of algorithm and accelerate the convergence of optimization.

Partition A partition of the volume is introduced to decrease the negative effects of the transition regions (which can not guarantee to be $C2$ continuous) and further reduce the computational complexity by setting a same T_i to the control points in each part Ω_i of the partition. Specifically, we initially calculate a stress field of $\mathcal{M}$ using the FEM finite element library [47] (Fig. 1a). Then, a stress-field-guided volume partition $\{\Omega_i\}_{i=1}^n$ of the model is obtained, as shown in Fig. 1b. In order to reduce the impact by transition regions, there are two reference constraint conditions: (1) avoiding excessive partition and (2) reducing border areas of the partition. Note that the number of partitions is set according to the complexity of models and stress map ($n = 2, 3$ or 4 for most models in our experiment), and the partition can be achieved using the modified K-means [48]. Also, a small number of user interactions are also supported (optional).

4.2 The formulation of lightweight problem

Based on the above conditions, the lightweight problem can be formulated into a constrained optimization with two types of parameters $\{T_i\}$ and O, in which case the lightweight model is the lightest weight while can withstand the given conditions

$$\begin{aligned} &\min_{\{T_i\},O} \mathcal{V}(T_i, O) \\ \text{s.t.} \quad &\max_{\sigma_s \in \mathrm{SM}(\tilde{\mathcal{M}}, f)} \sigma_s < \mathcal{Y}, \\ &T(c_j) = T_i, c_j \in \Omega_i, \end{aligned} \tag{8}$$

where $\mathcal{V}(*, *)$ is the volume of the interior porous structures, $\mathrm{SM}(\tilde{\mathcal{M}}, f)$ is a stress map (stress field) calculated on the model $\tilde{\mathcal{M}}$ with porous structures under the forces condition f (external forces and gravity), $\mathcal{Y}$ is the stress threshold related to the material (plastic PC-ABS material with $\mathcal{Y} = 41$ MPa is used by default), $\{c_j\}$ is the set of control points and $\{\Omega_i\}$ is the partition of the interior volume.

4.3 Strength-to-weight optimization

Strategy In this section, we exploit a strength-to-weight optimization to calculate the two parameters. We know that both the offset parameter and the period parameter have a similar influence on the strength (max stress) and the weight (volume rate) with monotonous regularity. Moreover, the period parameter has a larger variability and better optimization suitability than the offset parameter, and it is reasonable to first calculate a proper constant offset parameter and then optimize the period parameter according to the obtained offset parameter and the given constraints. Therefore, the optimization process consists of two local loops: the optimization of the offset parameter O and the optimization of the period parameter $\{T_i\}$. On account of the monotonicity of the parameters O and $T(*)$, the optimization can achieve the global approximation without local minima in very few iterations.

Optimization of the offset parameter In the former loop, we first optimize the parameter O by an uniform porous structure. It means that $T(\mathrm{r}) \equiv T^0$, where T^0 is decided by the shape of the given model, i.e., in order to maintain the connectivity of porous structures, there should be at least one period of the porous structures in the narrowest parts. Due to the monotonous influence on the strength-to-volume, we can easily obtain an optimized offset parameter O by solving the optimization in Eq. (8) using the well-known genetic algorithm [49].

Optimization of the period parameter In the later loop, we fix the optimized parameter O as a constant value, and the period parameter can also be optimized using simple heuristic algorithm due to its monotonous regularity. According to the previous partition, we have $\{(\Omega_1, T_1^0), (\Omega_2, T_2^0), \ldots, (\Omega_1, T_2^0)\}$, where $T_i^0 = T^0, 0 < i \leq n$, and n is the number of partition regions. We compute the updated stress map $\mathrm{SM}(\tilde{M}^0, f)$ of the current model $\tilde{M}^0$. There are three types of partition regions $\{\Omega_i\}$:

- *Case 1* There are some regions $\{\Omega_i\}$, in which the max stress is less than 90% of the threshold $\mathcal{Y}$ according to the current stress map. In this case, we update parameters of the corresponding regions by $T_i^{k+1} = T_i^k + \delta_k$, where $\delta_k = (T_i^k + 2)/2T_i^k - T_i^k$, then update the stress map $\mathrm{SM}(\tilde{M}^{k+1}, f)$ of the current model $\tilde{M}^{k+1}$;
- *Case 2* There are some regions $\{\Omega_i\}$, in which the max stress is larger than the given threshold $\mathcal{Y}$ according to the current stress map. In this case, we update parameters of the corresponding regions by $T_i^{k+1} = T_i^k - \delta_k$, where $\delta_k = T_i^k - 2T_i^k/(T_i^k + 2)$ is the step size, and then update the stress map $\mathrm{SM}(\tilde{M}^{k+1}, f)$ of the current model $\tilde{M}^{k+1}$;
- *Case 3* There is no region to satisfy Cases 1 or 2, and then we obtain the finial optimized period parameter $\{T_i^*\}$.

5 Experimental results and discussion

To be convenient for explanation and visualization, all the models in our experiments are filled using P surface-based porous structures, and the max size is set to 10 cm. Both external forces and gravity are considered, and all the experiments are conducted on a 3.4 GHz Intel(R) Core(TM) i7 computer with 32 G memory. The maximum length of bounding boxes of the models is set to 10 cm by default (except for Taurus is 5 cm, Shark, Fertility and Kitten are 15 cm). The thickness of the external shell is set according to the manufacturing accuracy (0.2 mm for the common FDM 3D printers), and we simply fix the external shell thickness to an uniform value (1 mm by default) in all our experiments.

5.1 Parameter selection

There are several parameters in our lightweight framework; however, most of them (such as α in Eq. 6, m in Eq. 4, C in Eq. 1 and the number n of partitions) are fixed or set empirically. Only offset parameter O and period parameter $\{T_i\}$ are released to optimize the lightweight models. As mentioned in the previous section, both the two parameters have the similar influence on the strength-to-weight ratio, and $\{T_i\}$ have a larger available range of changes than O according to the connectivity and the actual printable conditions. Therefore, the offset parameter O is considered to be a constant that will be first calculated using the optimization in Eq. (8), and users-specified offset is also allowed (we choose the former

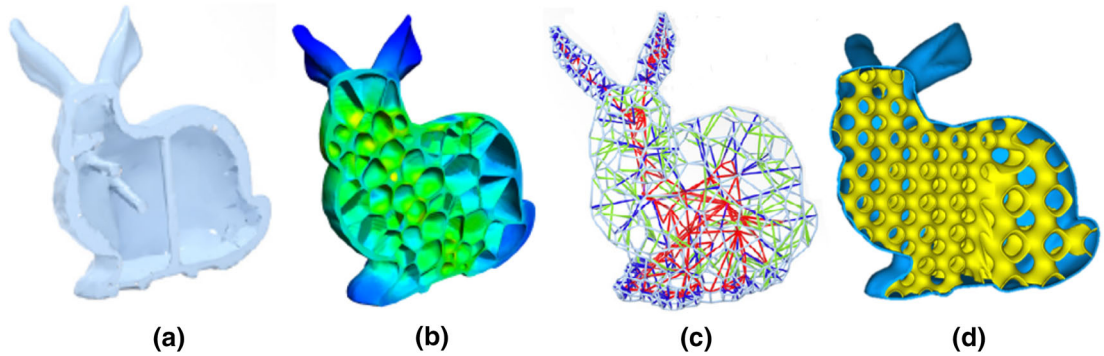

Fig. 6 Comparing with the most related methods. **a** Stava's method [1]. **b** Lu's method [2]. **c** Zhang's method [4]. **d** Our method provides comparable results with lighter, fully connected and quasi-self-supported porous structures

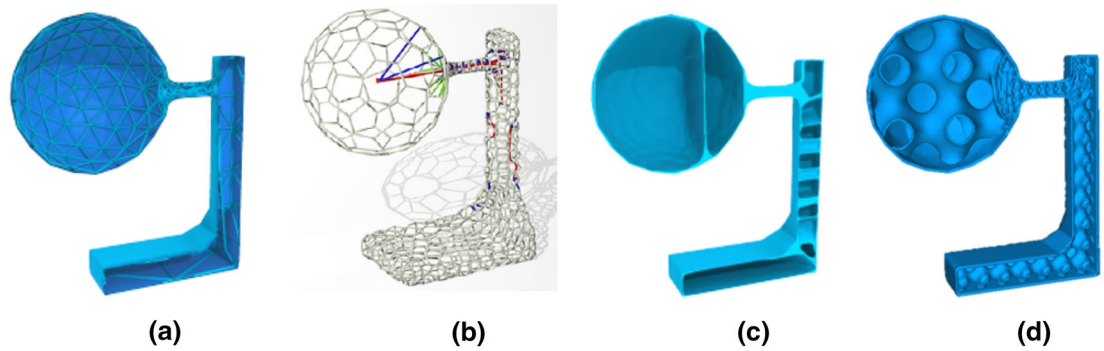

Fig. 7 In comparison with the skin-frame structure [3] (**a**), and the MA Tree structure [4] (**b**), the honeycomb-like structure [2] (**c**), our structure (**d**) is lighter than (**a**) and (**b**) and comparable to (**c**)

in this approach). Then, the period parameter $\{T_i\}$ can be optimized with fixed O in an iterative way, which will converge in less than ten iterations for all the examples in our experiments.

5.2 Comparison and discussion

We compare our results with several related methods under the same conditions defined in the experiments. For the model *Bunny*, external force 500 N is applied on the top of the model with fixed bottom. As shown in Fig. 6, the mass of the model in Stava's method [1] was reduced to 84.3 g, the honeycomb-like structure in Lu's method [2] could be reduced to 59 g and the MA Tree structure in Zhang's method [4] could be further reduced to 45.9 g. Furthermore, the multi-scale structure in our method can be optimized to 43.7 g due to two main reasons: (1) The smooth porous structures are good for transmitting force and (2) the multi-scale property ensures a preferable optimization approximation. Moreover, our proposed porous structures have more satisfactory properties, such as full connectivity and quasi-self-supporting.

For the model *Hanging Ball* (as shown in Fig. 7), external force 5 N is applied on the top and the bottom of the model is fixed. The mass of the skin-frame structure in Wang's method [3] is 109.3 g, the MA Tree structure in Zhang's method [4] is 61.6 g, the honeycomb-like structure in Lu's method [2] is 92.5 g (with 20 N force) and the multi-scale porous structure in our method is 44.98 g. Our multi-scale structure is lighter than the skin-frame structure [3] and the MA Tree structure [4] and is comparable to the honeycomb-like structure in [2]. Note that our method has advantages on connectivity and 3D printability. More results of the lightweight models are shown in Fig. 8). Table 1 lists the weight reduction of the models under the applied forces and gravity.

To evaluate the practical usability and further improve the results of the optimization, we printed the models filled with multi-scale porous structures using FDM-based 3D printer with plastic PC-ABS material (elasticity modulus 1807 MPa; yield strength 41 MPa), as shown in Fig. 9. The results of 3D printing also verify that the multi-scale structures constructed in our framework are free of extra supports. We also execute the actual mechanics analysis of these printed models using RG1-5 microcomputer control electronic universal testing machine, check whether they match the simulation and give feedback on the optimized results.

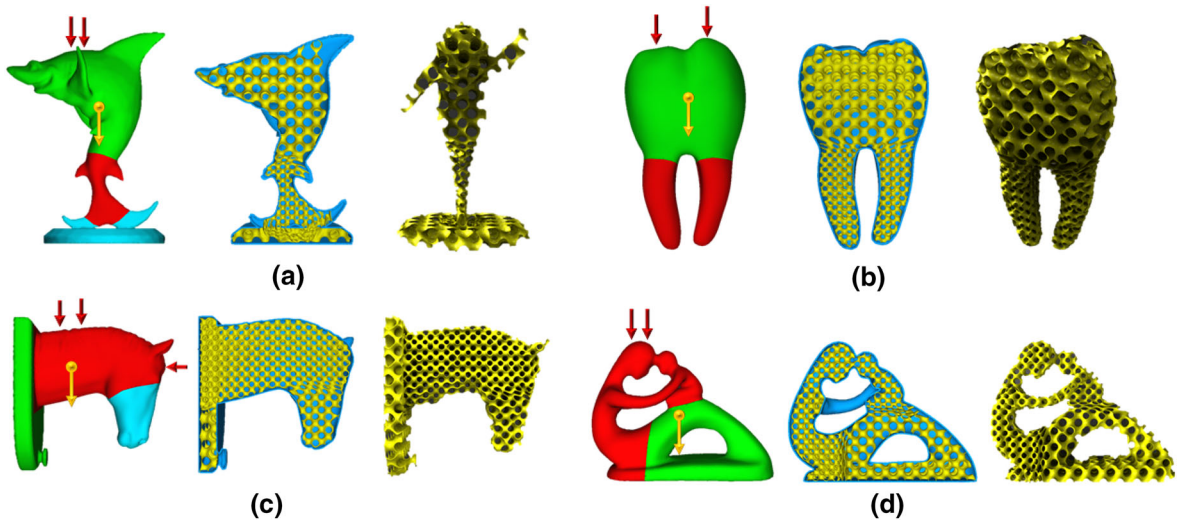

Fig. 8 More lightweight models filled with multi-scale porous structures. From left to right, original models with stress-field-guided partition, the optimal strength-to-weight results and the corresponding 3D multi-scale porous structures

Table 1 Optimization results for various models

Model	Force (N)	Porous shell vol. (cm^3)	Surface vol. (cm^3)	Total vol. (cm^3)	Solid vol.(cm^3)	Ratio (%)
Hanging ball	5	17.6	18.2	35.8	107.9	33.14
Shark	20	10.9	32.5	43.4	164.28	26.41
Fertility	80	33.9	37.9	71.8	217.3	33.04
Kitten	500	69.1	37.9	107.0	415.71	25.73
Bunny	500	18.6	15.2	33.8	102.5	32.98
Molar	500	17.8	14.7	32.5	114.1	28.51
Horse	1500	130.0	52.3	182.3	470.2	38.77

Fig. 9 Some printed lightweight models and the corresponding cross profiles

There still exist some challenges in our approach. The bottleneck of the optimization time is the computation of stress map using traditional finite element method, which relies heavily on the structural complexity and level. The total time for the optimization is about 1 h and on average of 50 min. We would like to explore more efficient porous representation and optimization method to accelerate our lightweight framework in our future work. Besides, our lightweight modeling does not guarantee a minima total weight since it is related to the volume partition. The partition should avoid over-segmentation because the transition regions between different parts negatively impact on the smoothness and full connectivity. In return, it provides a feasible approximation, which can achieve the global optimization under the formulation and converge fast.

6 Conclusion

In this approach, we propose a multi-scale porous structure-based lightweight framework to address the strength-to-weight problem of 3D objects, which could be fabricated using most of the common 3D printing technologies. Specifically, We construct a multi-scale porous structure utilizing TPMS and exploit the compactly supported radial basis functions interpolation to make the transition of the porous structures natural and smooth. Moreover, the multi-scale porous structures inherit the good properties of TPMS (such as smoothness, full connectivity and quasi-self-supporting). We formulate the lightweight problem into a strength-to-weight optimization and provide a feasible and efficient solution in few iterations. It also allows users to specify the density and the volume ratio of the porous structures. Various experiment results show the capability of our method. Compared with existing methods, our lightweight models can withstand external loads with smoother and lighter structures, and they are also suitable for most of the common 3D printing technologies.

Acknowledgements This research is supported by the National Natural Science Foundation of China Grant (61772104, 61432003, 2017YFB1103700, 2016YFB1101100, 61720106005 and DUT2017TB02).

Compliance with Ethical Standards

Conflict of interest The authors certify that there is no conflict of interest with any individual/organization for the present work.

References

1. Stava, O., Vanek, J., Benes, B., Carr, N., Měch, R.: Stress relief: improving structural strength of 3D printable objects. ACM Trans. Gr. **31**(4), 48:1–48:11 (2012)
2. Lin, L., Sharf, A., Zhao, H., Wei, Y., Fan, Q., Chen, X., Savoye, Y., Changhe, T., Cohen-Or, D., Chen, B.: Build-to-last: strength to weight 3d printed objects. ACM Trans. Gr. **33**(4), 97:1–97:10 (2014)
3. Wang, W., Wang, T., Yang, Z., Liu, L., Tong, X., Tong, W., Deng, J., Chen, F., Liu, X.: Cost-effective printing of 3d objects with skin-frame structures. ACM Trans. Gr. **32**(6), 177:1–177:10 (2013)
4. Zhang, X., Xia, Y., Wang, J., Yang, Z., Changhe, T., Wang, W.: Medial axis tree–an internal supporting structure for 3d printing. Comput. Aided Geom. Des. **35–36**, 149–162 (2015)
5. Melchels, F.P.W., Bertoldi, K., Gabbrielli, R., Velders, A.H., Feijen, J., Grijpma, D.W.: Mathematically defined tissue engineering scaffold architectures prepared by stereolithography. Biomaterials **31**(27), 6909–6916 (2010)
6. Rajagopalan, S., Robb, R.A.: Schwarz meets Schwann: design and fabrication of biomorphic tissue engineering scaffolds. Med. Image Comput. Comput.-Assist. Interv. **8**, 794–801 (2005)
7. Yoo, D.J.: Heterogeneous minimal surface porous scaffold design using the distance field and radial basis functions. Med. Eng. Phys. **34**(5), 625–639 (2012)
8. SHAPEWAYS. Tutorial: How to hollow objects for 3D printing. http://www.shapeways.com/tutorials/creating-hollow-objects.html
9. Rosen, D., Johnston, S., Reed, M.: Design of general lattice structures for lightweight and compliance applications. In: Rapid Manufacturing Conference, pp. 1–14 (2006)
10. Wang, H., Chen, Y., Rosen, D.W.: A hybrid geometric modeling method for large scale conformal cellular structures. In: ASME Computers and Information in Engineering Conference, Long Beach, CA, Sept, pp. 24–28 (2005)
11. Wang, T., Liu, Y., Liu, X.: Global stiffness structural optimization for 3D printing under unknown loads. J. Comput. Gr. Tech. **5**(3), 18–38 (2016)
12. Attene, M., Livesu, M., Lefebvre, S., Funkhouser, T.: Design, representations, and processing for additive manufacturing. Synth. Lect. Vis. Comput. Comput. Gr. Anim. Comput. Photogr. Imaging **10**, 1–146 (2018)
13. Martínez, J., Song, H., Dumas, J., De Lorraine, U., Lefebvre, S., De Lorraine, U.: Orthotropic k-nearest foams for additive manufacturing. ACM Trans. Gr. **36**(4), 1–12 (2017)
14. Hollister, S.J., Mater, N.: Porous scaffold design for tissue. Nat. Mater. **4**, 518–524 (2005)
15. Hutmacher, D.W.: Scaffolds in tissue engineering bone and cartilage. Biomaterials **21**, 2529–2543 (2000)
16. Schroeder, C., Regli, W.C., Shokoufandeh, A., Sun, W.: Computer-aided design of porous artifacts. Comput. Aided Des. **37**, 339–353 (2005)
17. Fryazinov, O., Vilbrandt, T., Pasko, A.: Multi-scale space-variant FRep cellular structures. Comput. Aided Des. **45**(1), 26–34 (2013)
18. Feng, J., Jianzhong, F., Lin, Z., Shang, C., Li, B.: A review of the design methods of complex topology structures for 3d printing. Vis. Comput. Ind. Biomed. Art **1**(1), 1–16 (2018)
19. Wang, Y.: Periodic surface modeling for computer aided nano design. Comput. Aided Des. **39**, 179–189 (2007)
20. Yang, N., Zhou, K.: Effective method for multi-scale gradient porous scaffold design and fabrication. Mater. Sci. Eng. C **43**, 502–505 (2014)
21. Li, D., Dai, N., Jiang, X., Chen, X.: Interior structural optimization based on the density-variable shape modeling of 3d printed objects. Int. J. Adv. Manuf. Technol. **83**, 1627–1635 (2015)
22. Savio, G., Meneghello, R., Concheri, G.: Design of variable thickness triply periodic surfaces for additive manufacturing. Prog. Addit. Manuf. (2019). https://doi.org/10.1007/s40964-019-00073-x
23. Cvijovi, D., Klinowski, J.: The t and clp families of triply periodic minimal surfaces. J. Phys. **I**(2), 137–147 (1992)

24. Restrepo, S., Ocampo, S., Ramírez-Romero, J.L.: Mechanical properties of ceramic structures based on triply periodic minimal surface (tpms) processed by 3d printing. J. Phys. Conf. Ser. **935**(1), 1–6 (2017)
25. Yoo, D.J.: Advanced projection image generation algorithm for fabrication of a tissue scaffold using volumetric distance field. Int. J. Precis. Eng. Manuf. **15**(10), 2117–2126 (2014)
26. Ruprecht, D., Müller, H.: Free form deformation with scattered data interpolation method. Geom. Modell. **281**, 267–281 (1993)
27. Li, D., Liao, W., Dai, N., Dong, G., Tang, Y., Xie, Y.M.: Optimal design and modeling of gyroid-based functionally graded cellular structures for additive manufacturing. Comput. Aided Des. **104**, 87–89 (2018)
28. Li, D., Dai, N., Tang, Y., Dong, G., Zhao, Y.: Design and optimization of graded cellular structures with triply periodic level surface-based topological shapes. J. Mech. Des. **7**(141), 1–13 (2019)
29. Wendland, H.: Piecewise polynomial, positive definite and compactly supported radial functions of minimal degree. In: Advances in Computational Mathematics, pp. 389–396. Springer, Berlin (1995)
30. Kailun, H., Jin, S., Wang, C.C.L.: Support slimming for single material based additive manufacturing. Comput. Aided Des. **65**, 1–10 (2015)
31. Zhou, Q., Panetta, J., Zorin, D.: Worst-case structural analysis. ACM Trans. Gr. **32**(4), 137:1–137:12 (2013)
32. Chai, S., Chen, B., Ji, M., Yang, Z., Lau, M., Xiao-ming, F.: Stress-oriented structural optimization for frame structures. Gr. Models **97**, 80–88 (2018)
33. Prévost, R., Whiting, E., Lefebvre, S., Sorkine-Hornung, O.: Make it stand: balancing shapes for 3d fabrication. ACM Trans. Gr. **32**(4), 81:1–81:10 (2013)
34. Wang, W., Liu, Y., Member, S., Jun, W., Tian, S.: Support-Free Hollowing. IEEE Trans. Vis. Comput. Gr. **24**(7), 2787–2798 (2017)
35. Xie, Y., Chen, X.: Support-free interior carving for 3d printing. Vis. Inform. **1**(1), 9–15 (2017)
36. Bächer, M., Whiting, E., Bickel, B., Sorkine-Hornung, O.: Spin-it: optimizing moment of inertia for spinnable objects. ACM Trans. Gr. **33**(4), 96:1–96:10 (2014)
37. Coros, S., Thomaszewski, B., Noris, G., Sueda, S., Forberg, M., Sumner, R.W., Matusik, W., Bickel, B.: Computational design of mechanical characters. ACM Trans. Gr. **32**(4), 83:1–83:12 (2013)
38. Wang, L., Whiting, E.: Buoyancy optimization for computational fabrication. Comput. Gr. Forum **35**(2), 49–58 (2016)
39. Skouras, M., Thomaszewski, B., Coros, S., Bickel, B., Gross, M.: Computational design of actuated deformable characters. ACM Trans. Gr. **32**(4), 82:1–82:10 (2013)
40. Jun, W., Dick, C., Westermann, R.: A system for high-resolution topology optimization. IEEE Trans. Vis. Comput. Gr. **22**, 1195–1208 (2016)
41. Bendse, M.P.: Optimal shape design as a material distribution problem. Struct. Optim. **1**(4), 193–202 (1989)
42. Wang, M.Y., Wang, X., Guo, D.: A level set method for structural topology optimization. Comput. Methods Appl. Mech. Eng. **192**(1–2), 227–246 (2003)
43. Xie, Y., Steven, G.: A simple evolutionary procedure for structural optimization. Comput. Struct **49**(5), 885–896 (1993)
44. Guo, X., Zhang, W., Zhong, W.: Doing topology optimization explicitly and geometrically-a new moving morphable components based framework. J. Appl. Mech. **34**(1), 255–282 (2014)
45. Wang, W., Li, B., Qin, S.: Cross section-based hollowing and structural enhancement. Vis. Comput. **33**, 949–960 (2017)
46. Wang, W., Qin, S., Lin, L.: Support-free frame structures. Comput. Gr. **66**, 154–161 (2017)
47. Patzák, B., Rypl, D.: Object-oriented, parallel finite element framework with dynamic load balancing. Adv. Eng. Softw. **47**(1), 35–50 (2012)
48. Wagstaff, K., Cardie, C., Rogers, S., Schrödl, S.: Constrained k-means clustering with background knowledge. In: Proceedings of the Eighteenth International Conference on Machine Learning, pp. 577–584 (2001)
49. Houck, C.R., Joines, J., Kay, M.G.: A genetic algorithm for function optimization: a matlab implementation. NCSU-IE-TR **95**(9), 1–10 (1995)

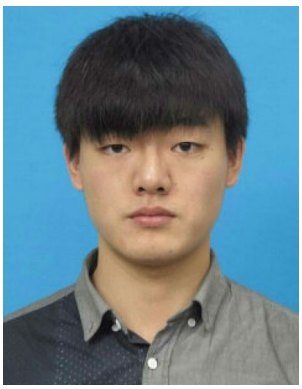

Jiangbei Hu is a Ph.D. candidate in School of Mathematical Sciences at Dalian University of Technology. He received the B.S. degree in applied mathematics from Dalian University of Technology in 2016. His research interests include computer graphics, 3D printing and mesh processing.

Shengfa Wang is an associate professor at DUT-RU International School of Information and Software Engineering and Key Laboratory for Ubiquitous Network and Service Software of Liaoning Province at Dalian University of Technology. He got his B.S. and Ph.D. in computational mathematics at Dalian University of Technology. His research interests include computer graphics, 3D printing, geometry processing and analysis.

Yi Wang is an associate professor at DUT-RU International School of Information and Software Engineering and Key Laboratory for Ubiquitous Network and Service Software of Liaoning Province at Dalian University of Technology. She received the B.S. and Ph.D. degrees in computer science and technology from Jilin University, Jilin, China, in 2002 and 2009, respectively. Her research interests include machine learning, deep learning, 3D printing and computer vision.

Fengqi Li is professorate senior engineer at School of software, Dalian University of Technology, China. He received the Ph.D. degree from the Dalian University of Technology. He is currently the director of public education of KAIFAQU Campus, Dalian University of Technology and the vice president of the Dalian Software Industry Association. His main interests include 3D printing, block chain and intelligent information system.

Zhongxuan Luo is a full professor in the School of Software at Dalian University of Technology, Institute of Artificial Intelligence at Guilin University of Electronic Technology. He got his B.S. in computational mathematics at Jilin University, M.S. in computational mathematics at Dalian University of Technology and Ph.D. in computational mathematics at Dalian University of Technology. His research interests are on computational geometry, computer graphics and image and computer-aided geometric design.